Inorg. Chem. **2007**, *46*, 510–516

Stabilization of Reduced Molybdenum–Iron–Sulfur Single- and Double-Cubane Clusters by Cyanide Ligation

Russell P. Pesavento, Curtis P. Berlinguette, and R. H. Holm*

Department of Chemistry and Chemical Biology, Harvard University, Cambridge, Massachusetts 02138

Received September 8, 2006

Recent work has shown that cyanide ligation increases the redox potentials of Fe_4S_4 clusters, enabling the isolation of $[Fe_4S_4(CN)_4]^{4-}$, the first synthetic Fe_4S_4 cluster obtained in the all-ferrous oxidation state (Scott, T. A.; Berlinguette, C. P.; Holm, R. H.; Zhou, H.-C. *Proc. Natl. Acad. Sci. U.S.A.* **2005**, *102*, 9741). The generality of reduced cluster stabilization has been examined with $MoFe_3S_4$ clusters. Reaction of single-cubane $[(Tp)MoFe_3S_4(PEt_3)_3]^{1+}$ and edge-bridged double-cubane $[(Tp)_2Mo_2Fe_6S_8(PEt_3)_4]$ with cyanide in acetonitrile affords $[(Tp)MoFe_3S_4(CN)_3]^{2-}$ (**2**) and $[(Tp)_2Mo_2Fe_6S_8(CN)_4]^{4-}$ (**5**), respectively. Reduction of **2** with $KC_{14}H_{10}$ yields $[(Tp)MoFe_3S_4(CN)_3]^{3-}$ (**3**). Clusters were isolated in ~70–90% yields as Et_4N^+ or Bu_4N^+ salts; clusters **3** and **5** contain all-ferrous cores, and **3** is the first $[MoFe_3S_4]^{1+}$ cluster isolated in substance. The structures of **2** and **3** are very similar; the volume of the reduced cluster core is slightly larger (2.5%), a usual effect upon reduction of cubane-type Fe_4S_4 and MFe_3S_4 clusters. Redox potentials and ^{57}Fe isomer shifts of $[(Tp)MoFe_3S_4L_3]^{2-,3-}$ and $[(Tp)_2Mo_2Fe_6S_8L_4]^{4-,3-}$ clusters with L = CN^-, PhS^-, halide, and PEt_3 are compared. Clusters with π-donor ligands (L = halide, PhS) exhibit larger isomer shifts and lower (more negative) redox potentials, while π-acceptor ligands (L = CN, PEt_3) induce smaller isomer shifts and higher (less-negative) redox potentials. When the potentials of **3**/**2** and $[(Tp)MoFe_3S_4(SPh)_3]^{3-/2-}$ are compared, cyanide stabilizes **3** by 270 mV versus the reduced thiolate cluster, commensurate with the 310 mV stabilization of $[Fe_4S_4(CN)_4]^{4-}$ versus $[Fe_4S_4(SPh)_4]^{4-}$ where four ligands differ. These results demonstrate the efficacy of cyanide stabilization of lower cluster oxidation states. (Tp = hydrotris(pyrazolyl)borate(1–)).

Introduction

The most significant feature of heterometallic cubane-type clusters $[L'L''MoFe_3S_4L_3]^z$ is an extensive redox capacity, encompassing the core oxidation states $[MoFe_3S_4]^{4+,3+,2+,1+}$. Their relative stability is highly dependent upon the terminal ligands L′, L″, and L at the six-coordinate molybdenum and tetrahedral iron sites, respectively. Very few clusters exhibit the full four-member electron-transfer series,[1] and the most oxidized member, produced at very positive potentials, has only been observed electrochemically. Stability is biased toward the other three members, such that redox series 1 is of practical synthetic and electrochemical importance.[2] However, the all-ferrous state $[MoFe_3S_4]^{1+}$, containing $Mo^{III} + 3Fe^{II}$, has never been isolated. Reductive coupling of single-cubane (SC) clusters affords the edge-bridged double-cubane (EBDC) clusters $[L'_2L''_2MoFe_6S_8L_4]^z$,[1,3,4] which contain the $Mo_2Fe_6S_8 = Mo_2Fe_6(\mu_3\text{-}S)_6(\mu_4\text{-}S)_2$ centrosymmetric core. In many clusters, L′ = Cl_4cat[5] and L″ = PR_3, solvate, or another unidentate ligand or L′ = Tp (L″ absent). Examples of SC and EBDC clusters are present in Figure 1. Combinations of the SC oxidation states $[MoFe_3S_4]^{2+,1+}$ have been stabilized in the EBDC geometry and are linked in redox series 2. Clusters in the 4+,[2,3,6–9] 3+,[2,9,10] and 2+[2,4,9] states have been isolated. A fourth oxidation state, [Mo_2-

* To whom correspondence should be addressed. E-mail: holm@chemistry.harvard.edu.

(1) Osterloh, F.; Segal, B. M.; Achim, C.; Holm, R. H. *Inorg. Chem.* **2000**, *39*, 980−989.
(2) Berlinguette, C. P.; Miyaji, T.; Zhang, Y.; Holm, R. H. *Inorg. Chem.* **2006**, *45*, 1997−2007.
(3) Demadis, K. D.; Campana, C. F.; Coucouvanis, D. *J. Am. Chem. Soc.* **1995**, *117*, 7832−7833.
(4) Zhang, Y.; Holm, R. H. *J. Am. Chem. Soc.* **2003**, *125*, 3910−3920.
(5) Abbreviations are given in Chart 1.
(6) Han, J.; Koutmos, M.; Al-Ahmad, S.; Coucouvanis, D. *Inorg. Chem.* **2001**, *40*, 5985−5999.
(7) Koutmos, M.; Coucouvanis, D. *Inorg. Chem.* **2004**, *43*, 6508−6510.
(8) Koutmos, M.; Georgakaki, I. P.; Coucouvanis, D. *Inorg. Chem.* **2006**, *45*, 3648−3656.
(9) Zhang, Y.; Holm, R. H. *Inorg. Chem.* **2004**, *43*, 674−682.
(10) Osterloh, F.; Achim, C.; Holm, R. H. *Inorg. Chem.* **2001**, *40*, 224−232.

10.1021/ic061704y CCC: $37.00
Published on Web 12/22/2006

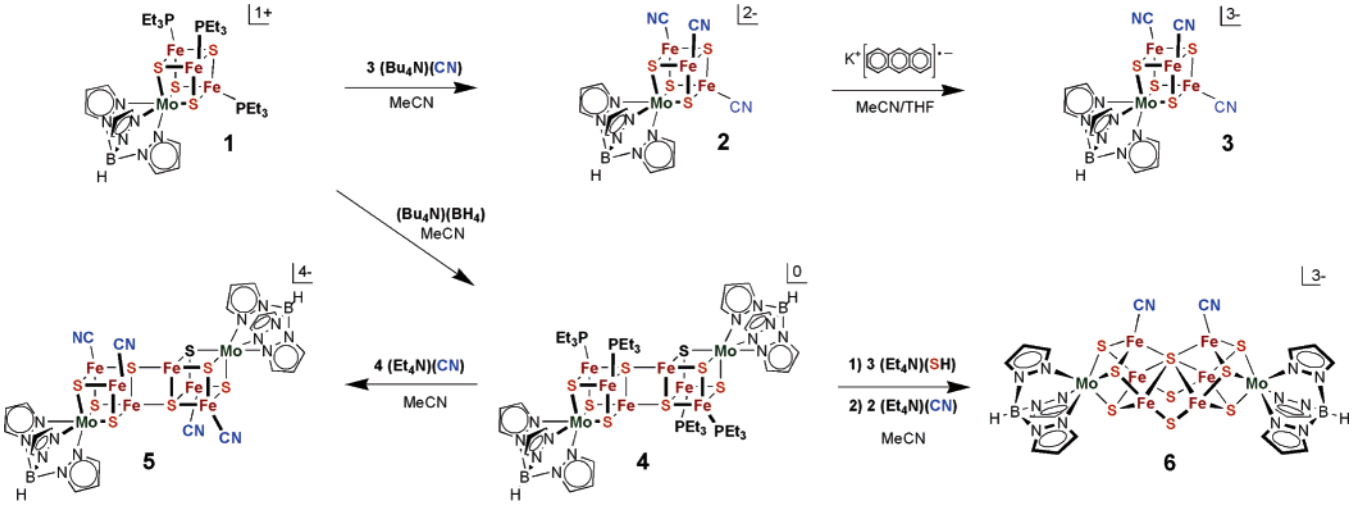

Figure 1. Scheme showing the synthesis of cyanide single cubane (**2**, **3**), edge-bridged double cubane (**5**), and P^N-type (**6**) clusters from phosphine clusters **1** and **4**.

$Fe_6S_8]^{5+}$, has been noticed electrochemically but is too unstable to isolate.[2]

$$[MoFe_3S_4]^{1+} \leftrightarrow [MoFe_3S_4]^{2+} \leftrightarrow [MoFe_3S_4]^{3+} \quad (1)$$

$$[Mo_2Fe_6S_8]^{2+} \leftrightarrow [Mo_2Fe_6S_8]^{3+} \leftrightarrow [Mo_2Fe_6S_8]^{4+} \quad (2)$$

The reactivity of the SC and EBDC clusters as precursors to other cluster species is dependent on the core oxidation state. For example, SCs form to EBDCs only when reduced below the $[MoFe_3S_4]^{3+}$ state,[3,4] and EBDCs in oxidation states below $[Mo_2Fe_6S_8]^{4+}$ and preferably $[Mo_2Fe_6S_8]^{2+}$ react with sulfide or selenide nucleophiles to form P^N-type clusters.[2,4,9,11] Consequently, we have continued our investigation of the ligand-modulated redox stability of both types of clusters with the goal of finding other species useful as precursors in the construction of weak-field clusters, with emphasis on those related to the P cluster and the MoFe-cofactor cluster of nitrogenase.[12] Recently, it has been established that the redox potentials of cubane-type Fe_4S_4 clusters are increased by means of cyanide ligation, facilitating the isolation of $[Fe_4S_4(CN)_4]^{4-}$, the first synthetic cluster obtained in substance in the all-ferrous $[Fe_4S_4]^0$ oxidation state.[13,14] In this work, we have examined the consequences of cyanide ligation on the stability of SC and EDBC clusters with L′ = Tp, thereby extending the scope of our recent study of SC and EBDC redox stabilities as dependent on terminal ligands L.[2]

Experimental Section

Preparation of Compounds. All reactions and manipulations were performed under a pure dinitrogen atmosphere using either Schlenk techniques or an inert atmosphere box. Solvents were passed through an Innovative Technology solvent purification system prior to use. Volume reduction and drying steps were carried out in vacuo. The compounds $(Et_4N)[(Tp)MoFe_3S_4Cl_3]$,[15] $[(Tp)MoFe_3S_4(PEt_3)_3](BPh_4)$, $[(Tp)_2Mo_2Fe_6S_8(PEt_3)_4]$, $(Et_4N)_3[(Tp)_2Mo_2Fe_6S_9(SH)_2]$,[4] and $(Et_4N)_3[(Tp)_2Mo_2Fe_6S_9(CN)_2]$[11] were prepared as described. Because of the small scale of the preparations, isolated compounds were not analyzed. They were characterized by three physical methods. The structures of the three compounds in Table 1 were determined by X-ray diffraction. Like other SC and EBDC $MoFe_3S_4$ clusters,[2,4,9,11] those obtained in this work display distinctive isotropically shifted ^1H NMR spectra, fully consistent with solid-state structures and satisfactory purity of isolated compounds. Parent ions with isotope distributions consistent with the formulations given were observed in electrospray mass spectra (M = cluster). In the following preparations, yields are based on the unsolvated formula weights of the cluster compounds.

$(Bu_4N)_2[(Tp)MoFe_3S_4(CN)_3]$. Method A. Ninety-four milligrams of $(Bu_4N)(CN)$ (0.35 mmol) dissolved in 2 mL of acetonitrile was added to 150 mg of $[(Tp)MoFe_3S_4(PEt)_3](BPh_4)$ (0.117 mmol) in 4 mL of acetonitrile. The black-brown solution was stirred for 1 h and reduced to one-half the original volume.

Table 1. Crystallographic Data for Compounds Containing the Clusters $[(Tp)MoFe_3S_4(CN)_3]^{2-}$, $[(Tp)MoFe_3S_4(CN)_3]^{3-}$, and $[(Tp)_2Mo_2Fe_6S_8(CN)_4]^{4-}$

	$(Bu_4N)_2$[**2**]	$(Et_4N)_3$[**3**]·MeCN	$(Et_4N)_4$[**5**]·6MeCN
formula	$C_{44}H_{82}BFe_3MoN_{11}S_4$	$C_{38}H_{73}BFe_3MoN_{13}S_4$	$C_{66}H_{118}B_2Fe_6Mo_2N_{26}S_8$
fw	1167.75	1116.22	2080.94
cryst syst	monoclinic	triclinic	triclinic
space group	$P2_1/n$	$P\bar{1}$	$P\bar{1}$
Z	4	2	1
a (Å)	11.189(2)	12.790(5)	12.022(5)
b (Å)	40.210(5)	13.476(7)	14.269(7)
c (Å)	12.596(3)	17.120(6)	15.744(8)
α (deg)	90	89.51(4)	112.40(4)
β (deg)	97.934(8)	75.03(3)	96.86(5)
γ (deg)	90	66.86(3)	107.08(4)
V (Å^3)	5613(2)	2607(2)	2304(2)
GOF (F^2)	1.045	1.051	1.090
R_1,[b] R_2[c]	0.054, 0.14	0.055, 0.15	0.058, 0.13

[a] Collected using Mo Kα radiation (λ = 0.71073Å) radiation at T = 213 K. [b] $R_1(F_o) = \sum[(F_o - F_o)]/\sum(F_o)$. [c] $R_2(F_o^2) = \{\sum[w(F_o^2 - F_c^2)^2/\sum[w(F_o^2)^2]\}^{1/2}$.

(11) Berlinguette, C. P.; Holm, R. H. *J. Am. Chem. Soc.* **2006**, *128*, 11993−12000.
(12) Lee, S. C.; Holm, R. H. *Chem. Rev.* **2004**, *104*, 1135−1157.
(13) Scott, T. A.; Zhou, H.-C. *Angew. Chem., Int. Ed.* **2004**, *43*, 5628−5631.
(14) Scott, T. A.; Berlinguette, C. P.; Holm, R. H.; Zhou, H.-C. *Proc. Natl. Acad. Sci. U.S.A.* **2005**, *102*, 9741−9744.
(15) Fomitchev, D. V.; McLauchlan, C. C.; Holm, R. H. *Inorg. Chem.* **2002**, *41*, 958−966.

Chart 1. Designation of Clusters and Abbreviations[a]

$[(Tp)MoFe_3S_4(PEt_3)_4]^{1+}$	**1**[4]
$[(Tp)MoFe_3S_4(CN)_3]^{2-}$	**2**
$[(Tp)MoFe_3S_4(CN)_3]^{3-}$	**3**
$[(Tp)_2Mo_2Fe_6S_8(PEt_3)_4]$	**4**[4]
$[(Tp)_2Mo_2Fe_6S_8(CN)_4]^{4-}$	**5**
$[(Tp)_2Mo_2Fe_6S_9(CN)_2]^{3-}$	**6**[11]

[a] Cl_4cat = tetrachlorocatecholate(2−), EBDC = edge-bridged double cubane, LS_3 = 1,3,5-tris((4,6-dimethyl-3-mercaptophenyl)thio)-2,4,6-tris(*p*-tolylthio)benzene(3-), SC = single cubane, Tp = hydrotris(pyrazolyl)borate(1−)

The careful addition of a layer of ether (85 mL) caused separation of the product as 128 mg (93%) of a black microcrystalline solid. ^{1}H NMR (CD_3CN, anion): δ 14.8 (br, 1), 14.04 (1), 6.33 (1). IR (KBr): 2038 cm^{-1} (ν_{CN}). ESMS: *m*/*z* 927.2 (calcd for $\{M + Bu_4N\}^-$ 927.0), 684.9 (calcd for $\{M\}^-$, 684.8), 658.9 (calcd for $\{M\text{-}CN\}^-$, 658.7), 342.6 (calcd for $\{M\}^{2-}$, 342.4).

Method B. The title compound can also be generated in situ by the addition of excess cyanide (5 equiv) to 1 equiv of $(Et_4N)[(Tp)MoFe_3S_4Cl_3]$ in an acetonitrile solution and stirring for 2−3 h. The yield is 70−80% based on the ^{1}H NMR spectra.

$(Et_4N)_3[(Tp)MoFe_3S_4(CN)_3]$ (3). A solution of 83 mg (0.54 mmol) of $(Et_4N)(CN)$ in 2 mL of acetonitrile was added to a solution of 100 mg (0.118 mmol) of $(Et_4N)[(Tp)MoFe_3S_4Cl_3]$ in 3 mL of acetonitrile to generate a black-brown solution. The reaction mixture was stirred for 2.5 h, and a freshly prepared solution of 0.023 g (0.207 mmol) of potassium anthracenide in THF was added to produce an initial deep blue solution that quickly converted to a black color. This solution was stirred for 15−20 min, filtered through Celite, and layered with 10 mL of ether. After 24 h, the product was collected as 92 mg (72%) of a black crystalline solid. ^{1}H NMR (CD_3CN, anion): δ 12.95(1), 11.7 (br, 1), 5.14(1). IR (KBr, cm^{1-}): 2059 (ν_{CN}). ESMS: *m*/*z* 1205.5 (calcd for $\{M + 4Et_4N\}^+$ 1205.4), 1075.3 (calcd for $\{M + 3Et_4N\}^+$, 1075.2).

$(Et_4N)_4[(Tp)_2Mo_2Fe_6S_8(CN)_4]$ (5). A solution of 44 mg (0.28 mmol) of $(Et_4N)(CN)$ in 3 mL of acetonitrile was added to a solution of 115 mg (0.068 mmol) of $[(Tp)_2Mo_2Fe_6S_8(PEt_3)_4]$ in 3 mL of acetonitrile. The black solution was stirred for 10 min, diluted with 0.2 mL of ether, and left to stand under an ether atmosphere overnight. The solid that separated was washed with 3 × 10 mL of acetonitrile to give the product as 106 mg (85%) of a black microcrystalline solid. ^{1}H NMR (CD_3CN, anion): δ 15.48(1), 14.15-(2), 10.15 (vbr, 1), 7.54 (vbr, 2), 4.74(2), 4.43(1). IR (KBr, cm^{-1}): 2086, 2059 (ν_{CN}). ESMS: *m*/*z* 1965.3 (calcd for $\{M + 5Et_4N\}^+$ 1965.3), 1836.1 (calcd for $\{M + 4Et_4N\}^+$ 1836.1), 1075.2 (calcd for $\{1/2\ M + CN + 3Et_4N\}^+$ 1075.2).

In the sections that follow, clusters are numerically designated according to Chart 1.**X-ray Structure Determinations.** Suitable crystals of $(Bu_4N)_2$[**2**], $(Et_4N)_3$[**3**]·MeCN, and $(Et_4N)_3$[**5**]·6MeCN were acquired by ether diffusion into an acetonitrile solution for at least 24 h. Crystals were coated with paratone-N oil and mounted on a Bruker APEX CCD-based diffractometer equipped with an LT-2 low-temperature apparatus operating at 213 K. Data were collected with scans of 0.3°/frame for 30 s, so that 1271−1850 frames were collected for a hemisphere of data. The first 50 frames were recollected at the end of the data collection to monitor for decay; no significant decay was detected for any compound. Cell parameters were retrieved with SMART software and refined using SAINT on all reflections. Data integration was performed with SAINT, which corrects for Lorenz polarization and decay. Absorption corrections were applied using SADABS. Space groups were assigned unambiguously by analysis of symmetry and systematic absences determined by XPREP.

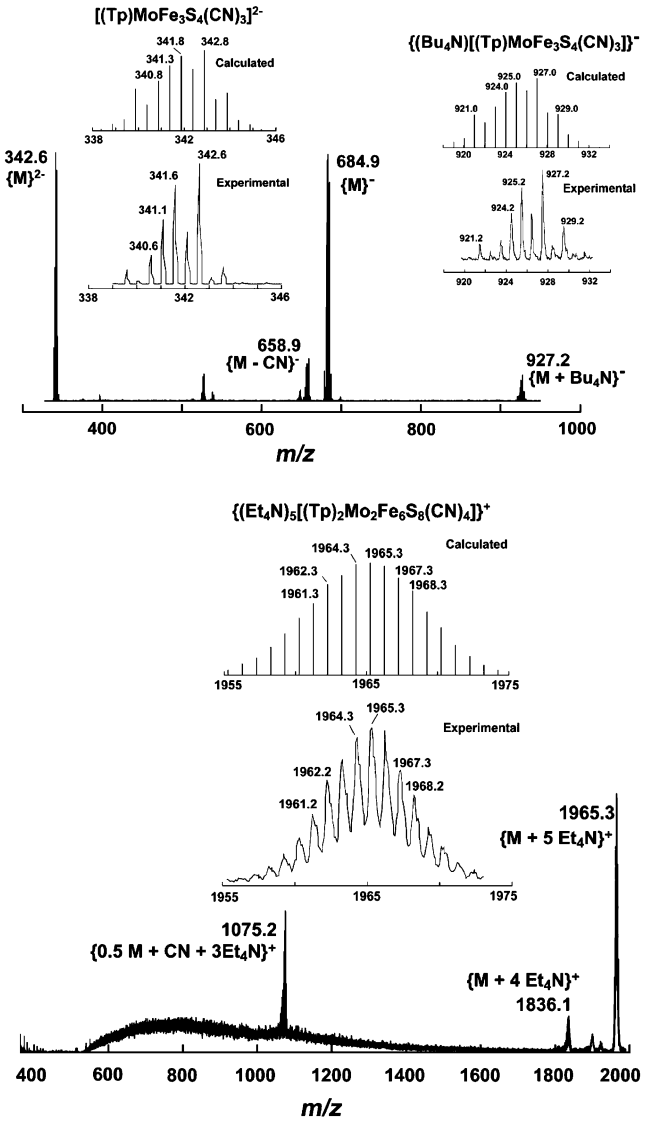

Figure 2. Experimental and calculated electrospray mass spectra of species containing the intact clusters $[(Tp)MoFe_3S_4(CN)_3]^{2-}$ and $[(Tp)_2Mo_2Fe_6S_8(CN)_4]^{4-}$.

The asymmetric unit of $(Bu_4N)_2$[**2**] consists of the cluster anion and two cations refined to full occupancy, and that of $(Et_4N)_3$[**3**]·MeCN contains the cluster anion, two cations at full occupancy, two cations at one-half occupancy, and one acetonitrile solvate molecule. In $(Et_4N)_4$[5]·6MeCN, the asymmetric unit includes one-half of the centrosymmetric cluster anion, two cations at full occupancy, and acetonitrile solvate molecules. Structures were solved by direct methods and refined against all data by full-matrix least-squares techniques on F^2 using the SHELXTL-97 package. All non-hydrogen atoms were refined anisotropically. Hydrogen atoms were placed at idealized positions on carbon atoms. Crystal parameters and agreement factors are reported in Table 1.[16]

Other Physical Measurements. All measurements were performed under anaerobic conditions. ^{1}H NMR spectra were obtained with a Varian AM-400 spectrometer. Electrochemical measurements were made with a Princeton Applied Research model 263 potentiostat/galvanostat using acetonitrile and solutions, a glassy carbon

(16) See paragraph at the end of this article for Supporting Information available.

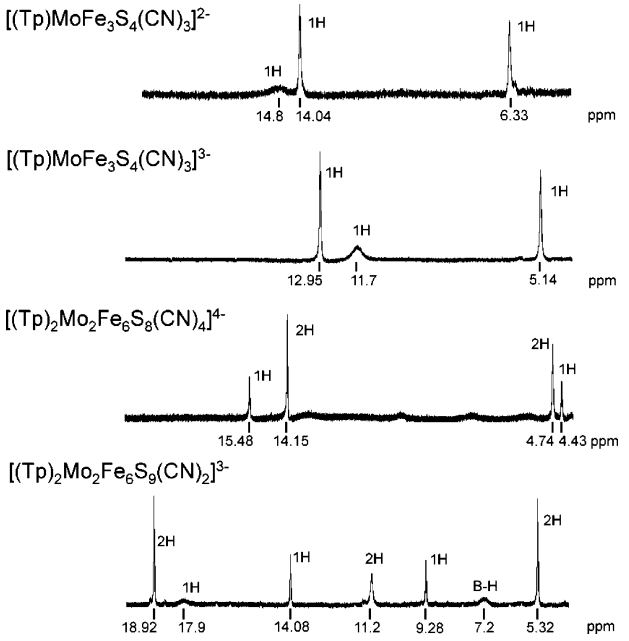

Figure 3. ^{1}H NMR spectra of cyanide clusters $[(Tp)MoFe_3S_4(CN)_3]^{2-,3-}$, $[(Tp)_2Mo_2Fe_6S_8(CN)_4]^{4-}$, and $[(Tp)_2Mo_2Fe_6S_9(CN)_2]^{3-}$ in CD_3CN solutions at room temperature. The EBDC was generated in solution because of the insolubility of the Et_4N^+ salt in acetonitrile.

working electrode, and 0.1 M $(Bu_4N)(PF_6)$ supporting electrolyte. Potentials are referenced to a standard calomel electrode (SCE). Electrospray mass spectra were recorded on acetonitrile and DMF solutions (∼1 mM) directly infused into a LCT mass spectrometer at a flow rate of 5 μL/min; experimental parameters are given elsewhere.[11] Infrared spectra were measured with a Nexus 470 FT-IR instrument. ^{57}Fe Mössbauer spectra were collected with a constant acceleration spectrometer. Data were analyzed using WMOSS software (WEB Research Corp., Edina, MN); isomer shifts are referenced to iron metal at room temperature

Results and Discussion

Cluster Synthesis and Characterization. An established entry point to diversely substituted single- and double-cubane clusters is ligand substitution of the phosphine clusters **1** and **4**.[2,4,9] Application of this procedure with cyanide in acetonitrile affords SC **2** (93%) and EBDC **5** (85%) in the indicated yields as black air-sensitive Bu_4N^+ and Et_4N^+ salts, respectively. Reduction of **2** generated in situ with excess potassium anthracenide afforded the Et_4N^+ salt of **3** (72%). All compounds were isolated as black air-sensitive solids. Clusters **2**, **3**, **5**, and the recently reported **6**,[11] a topological analogue of the P^N cluster of nitrogenase, comprise the current set of Tp- and cyanide-ligated Mo/Fe/S clusters. Cluster **3** is the first SC isolated in the $[MoFe_3S_4]^{1+}$ oxidation state.

Clusters were characterized by mass spectra, ^{1}H NMR, and X-ray structure determinations. The structural integrity of the cyanide clusters in solution was verified by low-resolution electrospray mass spectroscopy; selected spectra are depicted in Figure 2. In all cases, a parent ion species was observed in either positive or negative collection mode. For cluster **2**, the anions $\{(Bu_4N)[(Tp)MoFe_3S_4(CN)_3]\}^-$ (*m/z* 927.2) and $[(Tp)MoFe_3S_4(CN)_3]^{2-}$ (*m/z* 342.6) were observed, along with the monoanion ($[(Tp)MoFe_3S_4(CN)_3]^-$) (*m/z* 684.9). For cluster **3**, the species $\{(Et_4N)_4[(Tp)MoFe_3S_4(CN)_3]\}^+$ (*m/z* 1205.5) and $\{(Et_4N)_3[(Tp)MoFe_3S_4(CN)_3]\}^+$ (*m/z* 1075.3) were detected. The parent cation $\{(Et_4N)_5[(Tp)_2Mo_2Fe_6S_8(CN)_4]\}^+$ was observed at 1965.3 *m/z* for **5**, as well as an oxidation product containing **2**, corresponding to $\{(Et_4N)_3[TpMoFe_3S_4(CN)_3]\}^+$ (*m/z* 1075.2).

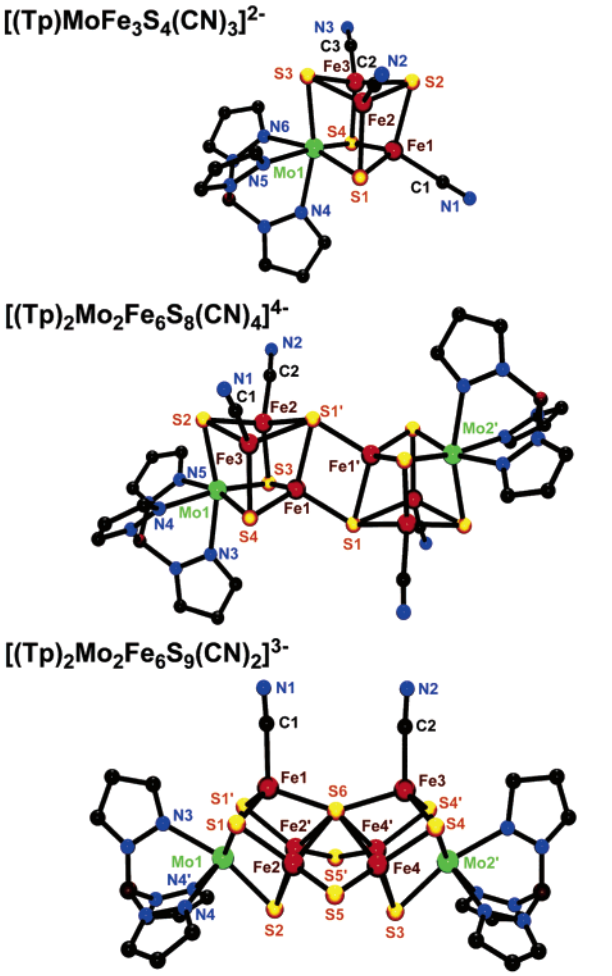

Figure 4. X-ray structures of $[(Tp)MoFe_3S_4(CN)_3]^{2-}$, $[(Tp)_2Mo_2Fe_6S_8(CN)_4]^{4-}$, and $[(Tp)_2Mo_2Fe_6S_9(CN)_2]^{3-}$ showing partial atom-labeling schemes. Primed and unprimed atoms in the middle and lower structures are related by a crystallographically imposed inversion center and mirror plane, respectively.

The ^{1}H NMR spectra of the set of four cyanide clusters are presented in Figure 3. Previous work has shown that the chemical shifts of pyrazolyl ring protons in SCs and EBDCs, isotropically shifted because of cluster paramagnetism, are quite sensitive to terminal ligands L.[2] The spectra of **2** and **3** show three equivalent pyrazolyl rings, consistent with C_{3v} symmetry. Reduced cluster **3** is converted to **2** upon standing or upon treatment with 1 equiv of $[(C_5Me_5)_2Fe]^+$. Cluster **5**, generated in situ, shows four well-resolved signals in a 2:1 intensity ratio, consistent with two inequivalent rings in the EBDC structure. The remaining two signals are apparently broadened beyond clear detection by cluster paramagnetism. In comparison, all signals of the two inequivalent equivalent rings of P^N-type cluster **6** are well-resolved. The spectra of **3** and **5** are the first recorded for all-ferrous SC and EBDC clusters with anionic ligands. Although several

Table 2. Selected Mean Bond Lengths (Å) and Volumes (Å^3) of Cyanide-Ligated Clusters

	$[(Tp)MoFe_3S_3(CN)_3]^{2-}$	$[(Tp)MoFe_3S_3(CN)_3]^{3-}$	$[(Tp)_2Mo_2Fe_6S_8(CN)_4]^{4-}$
Mo−S[a]	2.36(1)	2.37(1)	2.379(9)
Fe−S	2.26(4)[b]	2.27(3)[b]	2.28(1)[c], 2.40(2),[a,d] 2.255(2)[e]
Mo···Fe[a]	2.697(1)	2.72(2)	2.718(9)
Fe···Fe[a]	2.64(1)	2.686(6)	2.61(1), 2.827(3)[f]
Fe−C[a]	2.02(1)	2.00(3)	2.049(1)
$V(MoFe_3)$[g]	2.24	2.32	2.22
$V(S_4)$[g]	5.66	5.66	6.22
$V(MoFe_3S_4)$[g]	9.15	9.38	9.39

[a] Mean of 3. [b] Mean of 9. [c] Mean of 6. [d] Fe(1−3)−S1. [e] Fe1−S1′. [f] Fe1−Fe1′. [g] Additional volume data in the following order: $[(Tp)MoFe_3S_4Cl_3]^{1-}$ − 2.38, 5.54, 9.50 Å^3; $[(Tp)MoFe_3S_4Cl_3]^{2-}$ − 2.39, 5.73, 9.60 Å^3.

$[(Tp)_2Mo_2Fe_6S_8L_4]^{4-}$ clusters with L = halide or azide have been crystallized,[2,4,9] they are extremely easily oxidized in solution, and the spectra of $[(Tp)_2Mo_2Fe_6S_8L_4]^{3-}$ were obtained.[2] All spectra are consistent with the solid-state structures described below.

Cluster Structures. The structures of clusters **2**, **5**, and **6** are presented in Figure 4; metric data in the form of mean bond distances and core volumes are listed in Table 2. In all cases, cyanide functions as a terminal ligand, and the Fe−C≡N groups are nearly linear. Because the structures of numerous $MoFe_3S_4$ SCs,[12,17,18] including those with Tp ligation at the molybdenum site,[2,4,9,15] have been reported and the metric features of the clusters reported here are normal, no extensive discussion of these structures is required. The results in Figure 4 are provided as structure proofs. The structures of **2** and **3** (not shown) are practically identical and in this sense resemble the structures of another cluster pair, $[(Tp)MoFe_3S_4Cl_3]^{1-,2-}$,[15] that differ by one electron. A slight increase (∼3.8%) in the volume of the $MoFe_3S_4$ portion of the core, as calculated from atomic coordinates,[19] is noted. A small increase in core total volume upon reduction is normally observed, as with **2**/**3** (2.5%), $[(Tp)MoFe_3S_4Cl_3]^{1-,2-}$ (1.1%), and $[Fe_4S_4(CN)_4]^{3-,4-}$ (∼1%),[14] and presumably arises from the increased population of antibonding MOs with metal−sulfur character. Centrosymmetric cluster **5** is isostructural and essentially isodimensional with species such as $[(Tp)_2Mo_2Fe_6S_8L_4]^{4-}$ (L = F^-, Cl^-, N_3^-).

A prior X-ray study of the Et_4N^+ salt of **6** established atom connectivity but because of disorder problems refined only to R_1 = 13%.[11] Here we provide a structural depiction demonstrating that the cluster is a structural analogue of the P^N cluster of nitrogenase,[20,21] with the μ_6-S atom and a large external Fe−(μ_6-S)−Fe angle (143.0(3)°) being the most conspicuous features. Last, we note that terminal Fe−CN binding has been previously established in Fe_4S_4[13,14,22−24] and terminal Mo−CN binding in $MoFe_3S_4$[25−29] clusters, although only in the $[MoFe_3S_4]^{2+}$ oxidation state. In solution reactions, it was found that with labile ligands initially present at both iron and molybdenum sites, cyanide is bound first at the latter site.[26] The protective aspect of Tp−Mo ligation directs substitution to the iron sites, a feature necessary to the synthesis of EBDC and P^N-type clusters.

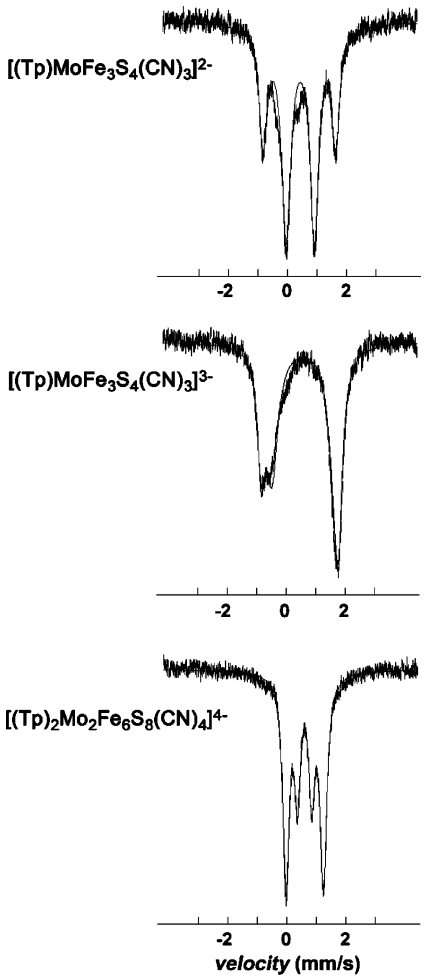

Figure 5. ^{57}Fe Mössbauer spectra of polycrystalline salts of the clusters $[(Tp)MoFe_3S_4(CN)_3]^{2-}$, $[(Tp)MoFe_3S_4(CN)_3]^{3-}$, and $[(Tp)_2Mo_2Fe_6S_8(CN)_4]^{4-}$ at 4.2 K in zero field. Solid lines are fits to the data using the parameters of Table 3.

Isomer Shifts and Oxidation States. The ability to vary the terminal ligands L in a large set of clusters of essentially constant structure provides an opportunity to examine the

(17) Holm, R. H.; Simhon, E. D. In *Molybdenum Enzymes*; Spiro, T. G., Ed.; Wiley: New York, 1985; pp 1−87.
(18) Malinak, S. M.; Coucouvanis, D. *Prog. Inorg. Chem.* **2001**, *49*, 599−662.
(19) Kasper, J. S.; Lonsdale, K. In *International Tables for X-Ray Crystallography*; Kynoch: Birmingham, U.K., 1967; pp 36−49.
(20) Peters, J. W.; Stowell, M. H. B.; Soltis, S. M.; Finnegan, M. G.; Johnson, M. K.; Rees, D. C. *Biochemistry* **1997**, *36*, 1181−1187.
(21) Mayer, S. M.; Lawson, D. M.; Gormal, C. A.; Roe, S. M.; Smith, B. E. *J. Mol. Biol.* **1999**, *292*, 871−891.
(22) Weigel, J. A.; Srivastava, K. K. P.; Day, E. P.; Münck, E.; Holm, R. H. *J. Am. Chem. Soc.* **1990**, *112*, 8015−8023.
(23) Weigel, J. A.; Holm, R. H. *J. Am. Chem. Soc.* **1991**, *113*, 4184−4191.
(24) Zhou, C.; Holm, R. H. *Inorg. Chem.* **1997**, *36*, 4066−4077.
(25) Mascharak, P. K.; Armstrong, W. H.; Mizobe, Y.; Holm, R. H. *J. Am. Chem. Soc.* **1983**, *105*, 475−483.
(26) Palermo, R. E.; Holm, R. H. *J. Am. Chem. Soc.* **1983**, *105*, 4310−4318.
(27) Palermo, R. E.; Singh, R.; Bashkin, J. K.; Holm, R. H. *J. Am. Chem. Soc.* **1984**, *106*, 2600−2612.
(28) Demadis, K. D.; Chen, S.-J.; Coucouvanis, D. *Polyhedron* **1994**, *13*, 3147−3151.
(29) Demadis, K. D.; Coucouvanis, D. *Inorg. Chem.* **1995**, *34*, 436−448.

Table 3. Redox Potentials and ^{57}Fe Mössbauer Parameters for the Clusters $[(Tp)MoFe_3S_4L_3]^{1-,2-}$ and $[(Tp)_2Mo_2Fe_6S_8L_4]^{4-,0}$

	$E_{1/2}$ (V)[a]				
cluster	4−/3−	3−/2−	2−/1−	δ[b] (mm/s)	ΔE_Q[b] (mm/s)
$[(Tp)MoFe_3S_4Cl_3]^{1-}$		−1.64	−0.57[c]	0.51(2), 0.46(1)[d]	0.61(1), 1.09(2)
$[(Tp)MoFe_3S_4(SEt)_3]^{1-}$			−0.96[d]	0.39[d]	1.02
$[(Tp)MoFe_3S_4F_3]^{2-}$		−1.87	−0.73[c]	0.58(1), 0.65(2)[c]	0.53(1), 1.15(2)
$[(Tp)MoFe_3S_4Cl_3]^{2-}$		*e*		0.60(1), 0.61(2)[c]	0.51(1), 1.11(2)
$[(Tp)MoFe_3S_4(SPh)_3]^{2-}$		−1.76	−0.69[c]	0.52(2), 0.51(1)	0.84(2), 2.16(1)
$[(Tp)MoFe_3S_4(CN)_3]^{2-}$		−1.49	(−0.23)[g]	0.45(1), 0.48(2)	2.47(1), 0.96(2)
$[(Tp)MoFe_3S_4(PEt_3)_3]^{1+}$		−0.79[i]		0.33(1), 0.35(2)	2.17(1), 1.46(2)
$[(Tp)MoFe_3S_4(CN)_3]^{3-}$		*f*		0.47(1), 0.59(2)	2.63(1), 2.15(2)
$[(Tp)_2Mo_2Fe_6S_8F_4]^{4-}$	−1.65	−1.04	−0.38[c]	0.71[c]	0.86
$[(Tp)_2Mo_2Fe_6S_8Cl_4]^{4-}$	−1.42	−0.88	−0.28[c]	0.65(1), 0.74(2)[c]	0.45(1), 0.83(2)
$[(Tp)_2Mo_2Fe_6S_8(SPh)_4]^{3-}$	−1.57	−0.98	−0.38[c]		
$[(Tp)_2Mo_2Fe_6S_8(CN)_4]^{4-}$ [h]	−1.46	(−0.66)[g]		0.60(1), 0.61(2)	0.48(1), 1.30(2)
$[(Tp)_2Mo_2Fe_6S_8(PEt_3)_4]^{j}$	−0.83[c,i]			0.37(1), 0.44(2)	0.46(1), 1.16(2)

[a] Given vs SCE in acetonitrile at 298 K unless otherwise noted. [b] 4.2 K, ±0.02 mm/s, relative intensities of quadrupole doublets indicated in parenthesis. [c] Ref 2. [d] Ref 15. [e] Same as 1− cluster. [f] Same as 2− cluster 0/1+ couple. [g] Irreversible; $E_{p,a}$. [h] Potentials in DMF. [i] 0/1+ couple. [j] The isomer shifts for this compound are given incorrectly in ref 4.

effects of these ligands on electron distribution as sensed by the ^{57}Fe isomer shifts and on redox potentials. While in mononuclear iron chemistry numerous homoleptic $[FeL_4]^{2-}$ and a smaller number of $[FeL_4]^{1-}$ complexes are known, reversible redox reactions are limited. Further, complexes of the type $[FeL'_3L]^{2-}$ with variable L are largely unknown, presumably because of unfavorable kinetic labilities. The redox potentials and Mössbauer spectroscopic parameters for cyanide clusters **2**, **3**, and **5** and other SC and EBDC clusters with different anionic terminal ligands, for comparison purposes, are collected in Table 3 . Additional data for Tp-coordinated clusters of these types are available elsewhere.[2,4,15] Isomer shifts of a large number of single cubanes and double cubanes of different structural types have led to the conclusion that redox reactions effect changes in an electron population largely localized in the three iron atoms of a MFe_3S_4 unit and that the probable oxidation state of the heteroatom (Mo, V) is M^{3+}.[1,12,15,30,31]

The Mössbauer spectra for **2**, **3**, and **5** are shown in Figure 5. Those of **2** and **5** are particularly well resolved for these structure types and oxidation levels. These spectra, like those for nearly all other SCs and EBDCs, can be analyzed in terms of two (usually overlapping) quadrupole doublets. In the following considerations, weighted average isomer shifts are used. The difference of 0.08 mm/s between the isomer shifts of **2** and **3** is consistent with the latter being more reduced. This value is very similar to the ∼0.1 mm/s observed for $[Fe_4S_4]^{2+,1+}$ clusters with thiolate ligands.[32] Isomer shifts respond to changes in *one* ligand at tetrahedral iron sites. The series 3 is observed for tetrahedral FeS_3L sites in SCs with the $[MoFe_3S_4]^{2+}$ ($3Fe^{2.33+}$) oxidation level and also applies to EBDCs with the $[Mo_2Fe_6S_8]^{2+}$ ($6Fe^{2+}$) core in which the isomer shifts are 0.08−0.14 mm/s higher. On a relative basis in this series, π-donor ligands increase (larger isomer shifts) and π-acceptor ligands diminish (smaller chemical shifts) electron density at the iron nuclei. Crudely, the larger isomer shifts are associated with higher Fe^{2+} character. The order $Cl^- > RS^- > PR_3$ has also been observed for VFe_3S_4 clusters.[30]

$$\begin{array}{lccccccc} L = & F^- & \gtrsim & Cl^- & \gtrsim & N_3^- > & PhS^- > & CN^- > \quad PEt_3 \\ \delta_{av} = & 0.63 & & 0.61 & & 0.58 & 0.52 & 0.47 \quad 0.34\ \text{mm/s} \end{array} \qquad (3)$$

In acetonitrile, all SCs show chemically reversible 3−/2− redox couples ($i_{pc}/i_{pa} \approx 1$, series 1), and EBDCs display similarly reversible 4−/3− and 3−/2− couples (series 2). Further, most SCs support a well-defined 2−/1− couple. Clusters **2**/**3** show the 3−/2− couple at −1.49 V, but the 2−/1− step is irreversible. Cluster **5** shows the 4−/3− couple at −1.46 V; other redox steps are not reversible. By use of the 3−/2− potentials of SCs, the stability order 4 emerges, in which the range is 380 mV (i.e., the ease of oxidation

$$L = F^- < PhS^- < Cl^- < N_3^- < CN^- \qquad (4)$$

increases from cyanide to fluoride). The 4−/3− potentials of EBDCs generate a similar series except for the position of cyanide which occurs between PhS^- and Cl^-. In order 4, cyanide produces a 270 mV stabilization of **3** versus $[(Tp)MoFe_3S_4(SPh)_3]^{3-}$, comparable to 310 mV for $[Fe_4S_4(CN)_4]^{4-}$ ($E_{1/2}{}^{4-/3-} = -1.42$ V) versus $[Fe_4S_4(SPh)_4]^{4-}$ ($E_{1/2}{}^{4-/3-} = -1.73$ V) in acetonitrile.[14] The efficacy of cyanide ligation in stabilizing all-ferrous cores toward oxidation is evident. The first indication of the influence of cyanide binding on potentials was obtained from the site-specific substitution reactions 5 in which a single ligand is displaced.[23,24] The observed redox stability order $L' = PhS^-$

$$[Fe_4S_4(LS_3)Cl']^{2-} + L' \rightarrow [Fe_4S_4(LS_3)L']^{2-} + Cl^- \qquad (5)$$

$< Cl^- < CN^-$, consistent with series 4, spans a range of 90 mV in acetonitrile.[24] It may be noted that the more-negative redox potentials for any reaction are associated with the presence of π-donor ligands, with fluoride effecting both the largest isomer shifts and lowest redox potentials. The correlation is uneven, but for single cubanes, it does place cyanide near the end of series 3 and at the end position in series 4. Phosphine clusters **1** and **4** possess the lowest

(30) Hauser, C.; Bill, E.; Holm, R. H. *Inorg. Chem.* **2002**, *41*, 1615−1624.
(31) Christou, G.; Mascharak, P. K.; Armstrong, W. H.; Papaefthymiou, G. C.; Frankel, R. B.; Holm, R. H. *J. Am. Chem. Soc.* **1982**, *104*, 2820−2831.
(32) Rao, P. V.; Holm, R. H. *Chem. Rev.* **2004**, *104*, 527−559.

isomer shifts and highest potentials. Because of different cluster charges, PEt_3 is not placed in ligand stability order 4. Previously, we had observed that the double cubanes $[M_2Fe_6(\mu_3\text{-}SEt)_3(SEt)_6]^{3-}$ with variable M exhibited a trend in isomer shift paralleling that in redox potential.[33] Increases of the ferrous character of the core led to more negative redox potentials.

Formation of P^N-Type Clusters. In addition to scrutinizing the effect of cyanide ligation on redox stability, there was an additional issue that led to the present investigation. The cores of P^N-type clusters, exemplified by **6** (Figures 1 and 4), are of current interest as structural analogues of the P^N cluster of nitrogenase and possible progenitors of similar analogues of the $MoFe_7S_9X$ core (X = C, N, or O) of the FeMo-cofactor cluster.[34] The means and scope of the formation of P^N-type clusters, including the types of bridging atoms that can be incorporated, are yet to be elucidated.

The most effective method at present for the preparation of clusters with this topology is by the reaction of an EDBC with a strong anionic nucleophile.[4,9,35] The reaction of phosphine cluster **1** with hydrosulfide or hydroselenide affords $[(Tp)_2Mo_2Fe_6S_8Q(QH)_2]^{3-}$, which upon treatment with cyanide results in terminal ligand substitution to yield $[(Tp)_2Mo_2Fe_6S_8Q(CN)_2]^{3-}$ (Q = S (**6**), Se).[11] The reaction pathway is undefined, but present evidence indicates that the attacking nucleophile is incorporated within the core as a μ_2-Q atom. When this nucleophile is EtS^- or MeO^-, these species are assimilated in μ_2 positions.[9] Given that RS^-, RO^-, and CN^- are among the strongest nucleophiles (kinetics definition), an investigation of the reaction with cyanide under comparable conditions resulted in ligand substitution to give **5** in high yield. The formation of a P^N-type structure with cyanide would most likely implicate a symmetrical (C_{2v}) Fe−C(N)−Fe $\mu_2-\eta_C^2$ interaction. This is a recognized but infrequent cyanide bridging mode; linear or slightly bent M−C≡N−M and nonlinear M-(CN)-M $\mu_2-\eta_C^2\eta_N^1$ bridging are much more commonly encountered.[36] The first of these is incompatible with the P^N core, and the second, while structurally documented with second and third row metals,[37−39] has never been observed with iron and may also be unsuitable. The formation of P^N-type cores with non-sulfur nucleophiles as a means of introducing atom X in structural analogues of biological clusters is under investigation in this laboratory.

Acknowledgment. This research was supported by NIH Grant GM 28856

Supporting Information Available: X-ray crystallographic files in CIF format for the three compounds in Table 1, and thermal ellipsoid plots for **2**, **3**, and **5**. This material is available free of charge via the Internet at http://pubs.acs.org.

IC061704Y

(33) Cen, W.; Lee, S. C.; Li, J.; MacDonnell, F. M.; Holm, R. H. *J. Am. Chem. Soc.* **1993**, *115*, 9515−9523.
(34) Einsle, O.; Tezcan, F. A.; Andrade, S. L. A.; Schmid, B.; Yoshida, M.; Howard, J. B.; Rees, D. C. *Science* **2002**, *297*, 1696−1700.
(35) Zuo, J.-L.; Zhou, H.-C.; Holm, R. H. *Inorg. Chem.* **2003**, 4624−4631.
(36) Dunbar, K. R.; Heintz, R. A. *Prog. Inorg. Chem.* **1997**, *45*, 283−391.
(37) Deraniyagala, S. P.; Grundy, K. R. *Inorg. Chim. Acta* **1984**, *84*, 205−211.
(38) Bartley, S. L.; Bernstein, S. N.; Dunbar, K. R. *Inorg. Chim. Acta* **1993**, *213*, 213−231.
(39) Bera, J. K.; Szalay, P. S.; Dunbar, K. R. *Inorg. Chem.* **2002**, *41*, 3429−3436.